THE JOURNAL OF PHYSICAL CHEMISTRY B

Article

pubs.acs.org/JPCB

Ionized Trilysine: A Model System for Understanding the Nonrandom Structure of Poly-L-lysine and Lysine-Containing Motifs in Proteins

Daniel J. Verbaro,[†] Daniel Mathieu,[‡] Siobhan E. Toal,[†] Harald Schwalbe,[‡] and Reinhard Schweitzer-Stenner*,[†]

[†]Department of Chemistry, Drexel University, 3141 Chestnut Street, Philadelphia, Pennsylvania 19104, United States

[‡]Institute for Organic Chemistry and Chemical Biology, Center for Biomolecular Magnetic Resonance (BMRZ), Johann Wolfgang Goethe University, Max-von-Laue-Strasse 7, 60438 Frankfurt, Germany

Supporting Information

ABSTRACT: It is now well-established that different amino acid residues can exhibit different conformational distributions in the unfolded state of peptides and proteins. These conformational propensities can be modulated by nearest neighbors. In the current study, we combined vibrational and NMR spectroscopy to determine the conformational distributions of the central and C-terminal residues in trilysine peptides in aqueous solution. The study was motivated by earlier observations suggesting that interactions between ionized nearest neighbor residues can substantially change conformational propensities. We found that the central lysine residue predominantly adopts conformations that are located at the upper border of the upper left quadrant of the Ramachandran plot and the left border of the polyproline II region. We term this type of conformation deformed polyproline II (pPII^d). The structures of less populated subensembles of trilysine resemble are comparable with structures at the $i + 1$ position of type I and type II β-turns. For the C-terminal residue, however, we obtained a mixture of polyproline II, β-strand, and right-handed helical conformations, which is typical for lysine residues in alanine- and glycine-based peptides. Our data thus indicate that the terminal lysines modify and restrict the conformational distribution of the central lysine residue. DFT calculations for ionized trilysine and lysyllysyllysylglycine in vacuo indicate that the pPII^d is stabilized by a rather strong hydrogen bond between the NH_3^+ group of the central lysine and the carbonyl group of the C-terminal peptide. This intramolecular hydrogen bonding induces optical activity in the C-terminal CO stretching vibration, which leads to an unusual and relatively intense positive Cotton band. Additionally, we analyzed the amide I′ band profile of ionized triornithine in water. Ornithine is structurally similar to lysine in that its side chain is terminated with an amino group; however, the side chain of ornithine is shorter than lysine's side chain by one methylene group. We found that the conformational distribution of the central ornithine in this peptide must be very similar to that of the central lysine residue in trilysine. This suggests that the ionized ammonium group, which lysine and ornithine side chains have in common, is the main determinant of their conformational propensities at the central position in the respective tripeptides. The results of a DFT-based geometry optimization confirm this notion. In principle, our results suggest that lysine-rich segments in unfolded/disordered proteins and peptides can switch between different types of local order, i.e., an extended pPII^d-like conformation and transient turns. However, for longer polylysine segments nonlocal interactions between side chains might impede the formation of turns, thus enabling the formation of pPII^d-helix segments.

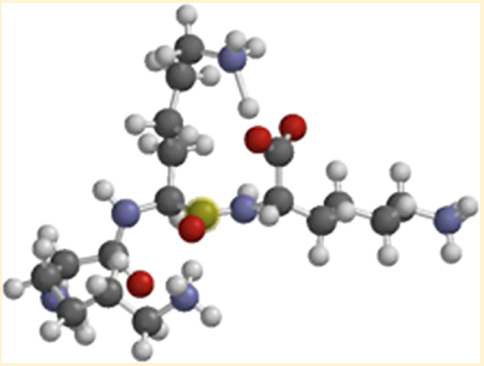

INTRODUCTION

It is now well-established that the unfolded state of peptides and proteins is not as conformationally random as suggested by the random coil model,[1−7] which basically assumes that each amino acid besides proline equally populates a rather broad region in the upper left quadrant of the Ramachandran plot ($-180° \le \Phi \le -50°$ and $90° \le \psi \le 180°$, region I), a slightly less extended trough located below the interface between upper and lower left quadrants ($-180° \le \Phi \le -30°$ and $-80° \le \psi \le 30°$; region II), and a more restricted one in the upper right quadrant ($60° \le \Phi \le 90°$ and $0° \le \psi \le 60°$, region III).[8−11] Numerous experimental data as well as results obtained from the analysis of truncated coil libraries suggest that most amino acid residues have a strong preference for region I, whereas region II is much less populated than predicted by the random coil model.[2,12−27] However, some amino acid residues, such as serine, cysteine, threonine, asparagine, and particularly aspartic acid, the side chains of which all can either donate or accept hydrogen bonding, do not belong in this category, owing to their relatively strong preference for structures that appear in various turns or can themselves be considered as turns.[18,28] Conformational analyses of short peptides further indicate that

Received: April 19, 2012
Revised: June 14, 2012
Published: June 19, 2012

dx.doi.org/10.1021/jp303794s | J. Phys. Chem. B 2012, 116, 8084−8094

region I contains at least two distinguishable subregions associated with polyproline II (pPII) and β-strand conformations ($-100° \leq \Phi \leq -60°$, $130° \leq \psi \leq 180°$ and $-180° \leq \Phi \leq -100°$, $90° \leq \psi \leq 180°$, respectively).[12,13,18,19,29−32] Different amino acid residues have been shown to exhibit different populations of pPII and β-strand. Alanine, for instance, has a very high propensity for pPII, whereas phenylalanine and valine have a higher preference for β-strand-like conformations.[19,33]

Besides alanine, ionized homopeptides like polylysine and polyglutamic acid have been identified as model systems for peptides with a predominant fraction of pPII-like conformations.[34−36] A somewhat different picture emerged from a recent UV-resonance Raman study on protonated polylysine from which the authors obtained a conformational mixture of nearly equal fractions of pPII and extended β-strand conformations. The latter was reported to exhibit a representative coordinate of $(\varphi, \psi) = (-130°, 170°)$ and was designated as a 2.5_1-helical conformation.[37] This result bears some similarity with the conformational distribution obtained for the central lysine residue in protonated GKG, i.e., 0.5 pPII and 0.41 extended β-strand with $(\varphi,\psi) = (-66°, 150°)$ and $(-115°, 145°)$ as representative coordinates, respectively.[19] For lysine in alanine-based peptides, we obtained mixtures of pPII, β-strand, and even right-handed helical conformations.[32] This discrepancy between reported distributions of isolated lysine in alanine/glycine-based host peptides and lysine in polylysine might be indicative of substantial nearest neighbor interactions between adjacent lysine or glutamic acid residues. A clarification of this issue is of general relevance owing to the frequent occurrence of lysine in functionally relevant disordered motifs and loops.[38−41] We therefore used a combination of vibrational and two-dimensional NMR spectroscopy to determine the conformational distribution of the central amino acid residue in ionized trilysine. Our results reveal a rather peculiar conformational distribution, which is clearly distinct from what we earlier obtained for the lysine residues in GKG, AAKA, and AAKAAAKA peptides.[19,21,42] A comparison with the structural distribution of triornithine reveals the ammonium group of lysine and ornithine as the common structural determinant for both peptides.

MATERIALS AND METHODS

Materials. Lysyllysyllysine (H-Lys-Lys-Lys-OH·acetate) was purchased from Bachem with >96% purity. No further purification was carried out. For the vibrational spectroscopy experiments, a peptide concentration of 0.2 M in D_2O (Sigma Aldrich) was prepared. The p*D* was adjusted with small aliquots of 35 w/w % DCl in D_2O (Sigma Aldrich). The pH was measured using an Accumet Research AR50 pH meter with an Accumet probe (Fisher Scientific). A p*D* value of 1.88 was calculated using the Glasoe and Long method.[43] We used very acidic conditions to facilitate the NMR measurements

For the electronic circular dichroism measurements, 0.01 M trilysine in 100% D_2O was prepared from a 0.2 M stock solution and sequentially titrated using small aliquots of DCl to obtain a p*D* of 1.86. Another sample was prepared at 0.01 M in 90% H_2O and 10% D_2O, and the sample was titrated with DCl until a p*D* of 1.91 was obtained.

For the measurements of the temperature dependence of the chemical shift of amide protons, a peptide concentration of 0.2 M in 10% D_2O/90% H_2O with TMS reference was prepared. The sample was titrated with DCl until a p*D* of 1.86 was obtained.

Uniformly $^{13}C/^{15}N$-labeled trilysine was synthesized using an Applied Biosystems ABI 433 peptide synthesizer following the standard Fmoc solid-phase synthesis protocol. Uniformly $^{13}C/^{15}N$-labeled α-N-Fmoc, $\sum$-N-tBoc protected lysine was purchased from Cambridge Isotope Laboratories Inc. Chlorotrityl resin and all coupling agents were purchased from NovaBiochem (Merck Chemicals). All solvents used were purchased from Sigma Aldrich at analytical grade. After synthesis, resin cleavage, and deprotection, the peptide was purified by reversed-phase HPLC chromatography. The purified peptide was freeze-dried and dissolved in 10% D_2O/90% H_2O with the pH adjusted to 2.

Ornithylornithylornithine (H-Orn-Orn-Orn-OH·acetate salt) was purchased from Bachem with >98% purity and no further purification was carried out. A peptide concentration of 0.2 M in D_2O was prepared. A p*D* of 1.96 was obtained by using small aliquots of DCl.

Methods. *Electronic Circular Dichroism.* Ultraviolet circular dichroism spectra were measured on a JASCO J-810 spectropolarimeter (JASCO, Inc.) purged with N_2. The 0.01 M sample was loaded into a 50 μm International Crystals Laboratories (ICL) cell. Spectra were measured between 180 nm and 300 nm with a 500 nm/min scan speed, a 1 s response time, a 0.05 data pitch, and a 5 nm bandwidth. Spectra were taken from 10 to 85 °C with 5 °C increments using a Peltier controller (model PTC-423S). All spectra were corrected using appropriate background subtraction.

Vibrational Spectroscopy. Infrared absorption and vibrational circular dichroism spectra were measured on a BioTools Chiral IR. Trilysine (0.2 M) was loaded into a 20 μm CaF_2 Biocell (BioTools). A BioTools water-cooled temperature controller was used to maintain a temperature of 25 °C. Spectra were taken with 4 cm^{-1} resolution and a total integration time of 840 min (756 min for VCD and 84 min for IR). All spectra were collected in Grams/AI 7.00 (Thermo Galactic). The absorbance spectrum was corrected with the subtraction of the appropriate background using Multifit. The same protocol was carried out for triornithine.

Polarized Raman spectra were taken on a Renishaw Ramascope with a confocal Olympus microscope. A Spectra-Physics argon/krypton ion laser was set to 514.5 nm, and the radiation was directed through a backscattering geometry using a notch filter. The 0.2 M trilysine was placed in a depression well microscope slide. A coverslip was carefully placed on top of the sample to minimize the presence of air bubbles. The microscope was focused past the coverslip and into the sample. Spectra were measured with scan times of 350 s for both parallel and perpendicular polarized light. Five accumulations were collected and averaged for each polarization. Spectra were measured at ambient temperature. Parallel and perpendicular polarized spectra were used to obtain anisotropic and isotropic scattering profiles.

NMR Spectroscopy. Homonuclear Coupling Constants. Amide proton $^3J(H^NH^\alpha)$ coupling constants were determined using ^1H NMR. The spectra were recorded on a Varian 500 MHz FT-NMR with a 5 mm HCN triple resonance probe. The temperature was controlled using a Varian VT controller, and spectra were taken between 25 and 65 °C in increments of 5 °C. The sample was allowed to equilibrate at each temperature for approximately 5 min before an experiment was started. Each spectrum was collected with 128 scans, and a PRESAT setting

dx.doi.org/10.1021/jp303794s | J. Phys. Chem. B 2012, 116, 8084−8094

was used to suppress the water. The FIDs were analyzed using Mestrec software, which was used to Fourier transform and phase the data. Then the raw data were analyzed in MultiFit.[44] The amide proton signals were decomposed using Lorentzian profiles with flexible half-widths. The same bandwidth was used for corresponding sub-bands of the decomposed doublets. The frequency positions of the peaks of the Lorentzian profiles were plotted as a function of temperature, and a linear regression in SigmaPlot was used to fit the data. The thus-obtained linear fitting equations were used to calculate the coupling constants as a function of temperature, as described in Toal et al.[45]

Heteronuclear Coupling Constants. Determination of φ- and ψ-dependent heteronuclear coupling constants has been carried out the same way as described previously.[19] The analysis has been done in accordance with Hagarman et al.[19] and Graf et al.[17] and references cited therein. All measurements were performed on a 400 MHz Bruker Avance II spectrometer equipped with an HCN-triple resonance probe with *z*-gradients. All measurements were done at a temperature of 298 K. Acquisition and processing has been done using Bruker Topspin version 2.1 using the same parameters as listed in Hagarman et al.[19] For the analysis of the *J*-modulated measurement of $^{n}J(\mathrm{NC}^{\alpha})$ (n = 1, 2) coupling constants, SigmaPlot 10 has been used.

RESULTS AND DISCUSSION

Conformational Analysis of KKK. We recently developed a protocol that allows us to obtain conformational distributions of amino acids in unfolded peptides from a combination of a variety of vibrational and NMR spectra.[31] With respect to the vibrational spectroscopies, we measured the amide I′ profile of the FT-IR, isotropic Raman, anisotropic Raman, and VCD spectra of the investigated peptides. Figure 1 shows these profiles for ionized trilysine. As observed for other tripeptides,[18,19,30,46] the amide I′ profiles are clearly asymmetric in IR and Raman spectra with peaks at 1650 and 1672 cm^{-1}. The higher wavenumber component overlaps with a broad band at 1712 cm^{-1}, which is attributed to the stretching vibration of the C-terminal carbonyl group (CO_s). Interestingly, the VCD spectrum indicates substantial rotational strength at the position of this band, which is normally not obtained owing to the absence of any vibrational coupling between amide I and CO_s.[47] For most tripeptides investigated thus far we observed a noncoincidence between the positions of maximal intensity of IR-absorption and isotropic Raman scattering, with the former at lower and the latter at higher wavenumbers.[18,19] The split is indicative of rather strong excitonic coupling found in (partially) extended conformations like pPII and β-strand.[48,49] Apparently, the profiles of trilysine do not exhibit this noncoincidence in that IR and Raman bands all exhibit the highest intensity at the position of the high-wavenumber band. This would normally be indicative of a helix-like conformation.[49] However, this notion would only be consistent with the very pronounced negative couplet, if we invoked a left-handed helix as the dominant conformation.[49−52] This seems to be a very unlikely option, since any helical structure should be disfavored for polylysine peptides owing to the repulsive Coulomb interactions between the protonated side chains. Indeed, the more quantitative analysis of our spectra described below reveals a different picture.

Table 1 lists the NMR coupling constants $^{3}J(\mathrm{H^{N}H^{\alpha}})$, $^{3}J(\mathrm{H^{N}C^{\beta}})$,$^{1}J(\mathrm{N,C^{\alpha}})$, $^{2}J(\mathrm{N,C^{\alpha}})$, and $^{3}J(\mathrm{H^{N}C^{\alpha}})$. The first two constants depend exclusively on φ, whereas the third and fourth ones depend on ψ. Since $^{2}J(\mathrm{N,C^{\alpha}})$ depends solely on the ψ-value of the preceding residue,[17,53] one would use, for example, the $^{2}J(\mathrm{N,C^{\alpha}})$ constant of the C-terminal peptide nitrogen as a

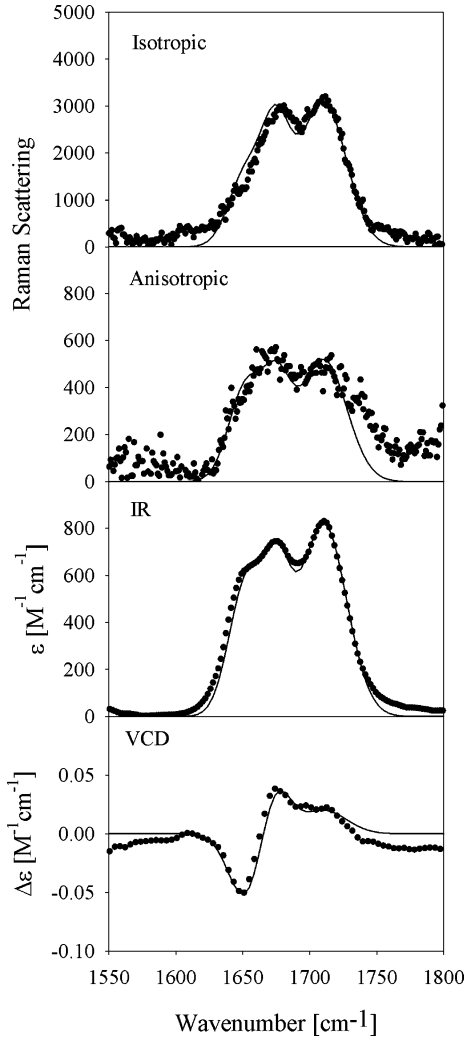

Figure 1. Amide I′ band profiles of fully protonated trilysine in D_2O. The experimental data (black dots) and simulation (black line) of the isotropic Raman (top panel), anisotropic Raman (second from top panel), IR absorption (third panel), and VCD (fourth panel) are depicted from 1550 to 1800 cm^{-1}. The experimental conditions and simulation parameters are described in the text.

Table 1. NMR Coupling Constants Are Listed with Associated Statistical Errors[a]

	Experimental central-terminal lysine coupling constants (Hz)	Calculated central-terminal lysine coupling constants (Hz)	Experimental C-terminal lysine coupling constants (Hz)	Calculated C-terminal lysine coupling constants (Hz)
$^{3}J(\mathrm{H^{N}H^{\alpha}})$	6.96 ± 0.02	6.84	6.00 ± 0.03	6.07
$^{3}J(\mathrm{H^{N}},\mathrm{C^{\beta}})$	1.28 ± 0.11	1.26	2.12 ± 0.18	2.08
$^{1}J(\mathrm{N,C^{\alpha}})$	10.96 ± 0.06	11.09	11.04 ± 0.08	11.00
$^{2}J(\mathrm{H^{N}C^{\alpha}})$[b]	8.41 ± 0.11	8.16		
$^{3}J(\mathrm{H^{N}C^{\alpha}})$			0.59 ± 0.11	0.49

[a]These constants were determined as described in the text. The calculated coupling constants were obtained from the amide I′ analysis of trilysine in 100% D_2O. [b]Note that $^{2}J(\mathrm{N,C^{\alpha}})$ is a C-terminal coupling constant that measures the central residue ψ-value.

dx.doi.org/10.1021/jp303794s | J. Phys. Chem. B 2012, 116, 8084−8094

measure of the ψ-angle of the central residue. Its Karplus parameters have a larger uncertainty than those of $^1J(N,C^\alpha)$.[53] The $^3J(H^NC^\alpha)$ constant was solely used for analyzing the C-terminal residue; its meaning is described below. In order to self-consistently reproduce these coupling constants and the amide I′ band profiles, we described the conformational distribution of the central K-residue as a superposition of statistically weighted two-dimensional Gaussian distributions as described in earlier publications.[18,19,31] The average $^3J(H^NH^\alpha)$, $^3J(H^NC^\beta)$, $^1J(N,C^\alpha)$, and $^2J(N,C^\alpha)$ coupling constants for this distribution were calculated. The amide I′ profiles in Figure 1 depend on this distribution, because excitonic coupling mixes the excited vibrational states of the two amide modes.[54] The coupling itself as well as its influence on IR, anisotropic Raman, and VCD profiles depends on the dihedral angles of the central residue.[30,54] For our simulations of the amide I′ profiles, the intrinsic frequency of the N-terminal band was set to 1676 cm^{-1}, and the intrinsic frequency of the C-terminal was set to 1653 cm^{-1} as studies on dipeptides indicate that the lower frequency band is attributed to the C-terminal amide.[55] These values are slightly different from the experimental values, since excitonic coupling increases the splitting between the two bands. They are also slightly (~3−5 cm^{-1}) higher than corresponding values of, e.g., trialanine or trivaline.[30] That might in part reflect the influence of the different side chains.[56] The profiles of the individual amide I′ bands were also assumed to be Gaussians. Their half-half-widths of 12.5 and 10.5 cm^{-1} for the N-terminal and the C-terminal bands, respectively, were obtained by a spectral decomposition of the amide I′ band profile with MultiFit. For the simulation of the IR and VCD profiles, the magnitude of the amide I′ dipole was obtained from Measey et al. as 3.3×10^{-19} esu cm.[56] The profile of the CO-band at 1711 cm^{-1} is also predominantly Gaussian with a half-width of 17.0 cm^{-1}. The experimental data-based optimization of the conformational distribution was carried out by using the center and the half-half-widths of two-dimensional Gaussian subdistributions and their respective statistical weights as free parameters. These parameters were varied until all amide I′ band profiles in Figure 1 and all *J*-coupling constants listed in Table 1 were simultaneously and satisfactorily reproduced. It should be noted that a magnetic transition dipole moment with a magnitude of 1.5×10^{-23} esu cm had to be assumed for the C-terminal amide I′ to account for the negative bias of the VCD couplet. This has emerged as a necessity for many peptides with a protonated C-terminal residue.[19,30,31,46,57] The physical reason for the existence of this magnetic moment has not yet been given.

The final result of our simulation of amide I profile is depicted by the solid lines in Figure 1. The high wavenumber band assignable to the CO-stretch was empirically modeled by a single Gaussian profile. The agreement between simulation and experimental data is excellent. The same can be said for the obtained *J*-coupling constants $^3J(H^NH^\alpha)$, $^3J(H^NC^\beta)$, and $^1J(N,C^\alpha)$. The calculated $^2J(N,C^\alpha)$ coupling constant of 7.93 Hz is slightly lower than the experimental value of 8.41 Hz. This is not surprising owing to the comparatively large uncertainty of the Karplus parameters for $^2J(N,C^\alpha)$.[53] A reproduction of this coupling constant would require that all ψ-values would be close to 180°, which would lead to an overestimation of $^1J(N,C^\alpha)$.

Our analysis is based on the assumption that the CO_s vibration is not coupled to the two amide I′ modes. This has been shown to be the case for trialanine by Woutersen and Hamm.[47] It is generally a very reasonable assumption since the wavenumber difference is too large for the C-terminal amide I′. For the N-terminal amide I, the spatial distance is too large to allow for a substantial mixing of states that are more than 40 cm^{-1} apart. However, one might be tempted to interpret the occurrence of a positive Cotton band at the CO_s position as indicative of excitonic coupling between CO_s and the C-terminal amide I′. If this was true the negative bias of the amide I′ VCD would be a result of this coupling. To check this possibility, we constructed a symmetric VCD amide I′ couplet the positive maximum of which matched the positive maximum of the experimental spectra and subtracted this hypothetical couplet from the experimental VCD amide I′ signal. The result is shown in Figure S1 of the Supporting Information. The remaining signal at the low-wavenumber amide I′ position is clearly less intense than the very broad positive maximum at the CO_s position. This shows that it is unlikely that the latter stems predominantly from excitonic coupling between CO_s and the C-terminal amide I, which would cause negative and positive signals of comparable strength. We therefore conclude that the observed rotational strength of CO_s reflects an intrinsic magnetic transition moment whose physical origin we will discuss below.

Figure 2 visualizes the conformational distribution obtained from this procedure. A major fraction of the peptide samples a

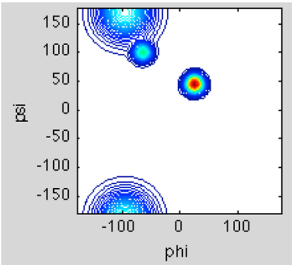

Figure 2. Contour plot of the conformational distribution of the central residue of trilysine in aqueous solution obtained from a combined analysis of amide I′ profiles and *J*-coupling constants described in the text.

Ramachandran subspace that lies above the canonical pPII and β-strand region. With respect to its φ-coordinate, this subspace is positioned at the left border of the pPII region defined in our earlier studies. The corresponding subdistribution overlaps with the lower region of the lower left quadrant of the Ramachandran plot. Since this distribution differs to a significant extent from classical pPII distributions centered in the vicinity of $(\varphi, \psi) = (-75°, 150°)$, we term the conformations of this subensemble $pPII^d$, where the superscript d means deformed. The $pPII^d$ fraction contains 71% of the entire ensemble. The remaining fraction of the obtained conformational ensemble, contain two subdistributions with statistical weights of 19.5% and 9.5%, which correspond to conformations found at the $i + 1$ position of type I′ and type II β-turns, respectively. Considering these turnlike conformations was essential for minimizing the differences between experimental and calculated *J*-coupling constants. It is important to emphasize that the turnlike conformations only represent part of a complete turn structure. A complete β-turn requires a hydrogen bond between the ith and $(i + 4)$th residue, which cannot be formed in tripeptides. This is a rather unusual distribution, which is distinct from what we have observed thus

dx.doi.org/10.1021/jp303794s | J. Phys. Chem. B 2012, 116, 8084−8094

far for other tripeptides, which with the exception of GDG contained rather canonical pPII subensembles.[18,19,28] It is also clearly distinct from anything that one would call a random coil. The parameter values of the obtained distribution are listed in Table 2.

Table 2. Populations of Conformers for the N-Terminal Lysine Considered for the Amide I′ Analysis as Described in the Text[a]

population (center)	mole fraction
pPII[d] (−95, 170)	0.710
β I′-turn (25, 45)	0.195
β II-turn (−65, 100)	0.095

[a]The center of the distribution is listed in parentheses.

It should be mentioned that the data could also be reproduced if we substituted the dominant subdistribution in the upper left quadrant by a bimodal subdistribution. The corresponding two Gaussian subdistribution each carry 35% of the total population. The respective coordinate of their maxima are $(\Phi, \psi) = (-90°, 180°)$ and $(\Phi, \psi) = (-120°, 170°)$. The corresponding fit to the amide I′ profiles is of a quality that is comparable with that shown in Figure 1. However, the *J*-coupling constants were slightly less well-reproduced. In the Ramachandran plot, these two distributions would overlap and appear as a very broad distribution, which is not qualitatively different from the above single pPII[d] distribution.

We also determined some coupling constants for the C-terminal, namely, $^3J(H^NH^\alpha)$, $^3J(H^NC^\beta)$, $^1J(NC^\alpha)$, and additionally $^3J(H^NC^\alpha)$, which are listed in Table 1. Assuming that the Karplus relations for these constants are also applicable for C-terminal residues (which has not yet been proven), we carried out a simulation that yielded the theoretical values listed in Table 1. The thus-obtained conformational distribution contains three Gaussians centered at classical pPII, β-strand, and (right-handed) helical coordinates (Table 3). The distribution is dominated by pPII.

Table 3. Populations of Conformers for the C-Terminal Lysine[a]

population (center)	mole fraction
pPII (−76, 145)	0.685
β-strand (−120, 120)	0.090
right-handed helical (−60, −30)	0.225

[a]These values were constrained by the associated coupling constants listed in Table 1. The center of the distribution is listed in parentheses.

Given that $^3J(H^NC^\alpha)$ depends on the φ-angle of the C-terminal residue and the ψ-angle of the central residue, we carried out another simulation that explicitly considers this relationship. To clarify, the φ-values listed in Table 3 and the ψ-values listed in Table 2 were coalesced into one ensemble. The φ- and ψ-values with similar weights were joined and the weights were averaged since the weights were not identical. The resulting $^3J(H^NC^\alpha)$ was 0.49, which is within the error of the measured value (0.59 ± 0.11). Even though, due to the limited data set, the analysis of the C-terminal residues is less reliable than that of the central terminal, it is safe to say that the C-terminal lysine shows a more conventional behavior with a large fraction of "normal" pPII. This distribution is similar to what we obtained earlier for lysine residues in GKG, AAKA, and $(AAKA)_2$.[19,42]

In order to shed some light on the forces that might cause the somewhat peculiar conformation distribution of the central lysine residue, we obtained an optimized geometry of the ionized KKK in vacuo by performing a DFT calculation on the B3LYP 6-31G** level of theory using the TITAN software package from Schrödinger, Inc. For this calculation the center of the above pPII[d] subdistribution was used as a starting point. Figure 3 displays the structure obtained from this procedure.

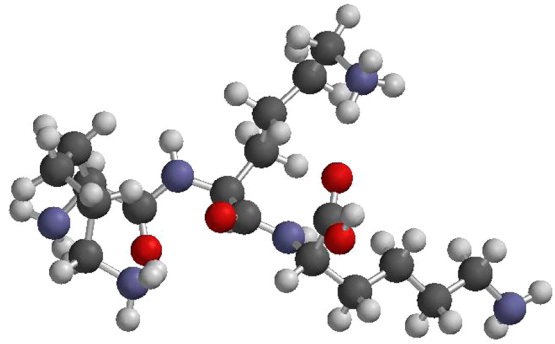

Figure 3. Structure of an unblocked KKK obtained by carrying out an in vacuo energy minimization with a DFT calculation on the B3LYP 6-31G** level of theory using the TITAN software package from Schrödinger, Inc. For this calculation, the center of the above pPII[d] subdistribution was used as the starting point.

The corresponding dihedral angles for the central residues are $(\Phi, \psi) = (-74°, 171°)$, which is close to the region of the pPII[d] subdistribution. The conformation in Figure 3a shows one of the side chain ammonium protons of the N-terminal residue in hydrogen-bonding distance to the corresponding peptide carbonyl (1.6 Å) and an ammonium proton of the central residue in hydrogen-bonding distance to the C-terminal carboxylate group. The attractive force associated with the latter interaction is so large that proton translocation is predicted to occur in vacuo. While this is unlikely to occur in an aqueous solution, our results suggest that hydrogen bonding between the ammonium groups and its partners could be strong enough to compete with hydrogen bonding to water molecules, thus stabilizing the pPII[d] structure. For the C-terminal, the above calculation yielded $(\Phi, \psi) = (-74°, 162°)$.

One might argue that the result of the DFT calculations reveals that the occurrence of pPII[d] is caused by a so-called end-effect with a terminal group, which would not occur in longer polylysine peptides. In order to check whether or not such intramolecular hydrogen bonding could still occur if the carboxylate group is replaced by an additional peptide group, we performed a DFT (B3LYP 6-31G**) based geometry optimization for the unblocked peptide KKKG. The above pPII[d] coordinates were used as starting points for the two central K-residues. The structure resulting from this procedure still exhibits the ammonium group of the second lysine in hydrogen-bonding distance to the carbonyl group of the C-terminal peptide group (2.3 Å, cf. Figure S2 of the Supporting Information). The dihedral angles obtained for the other two K-residues $[(\Phi, \psi) = (-91°, 173°)$ and $(-82°, 175°)]$ both lie in pPII[d] region. These results clearly demonstrate that our results for KKK can be considered as representative for longer polylysine peptides.

dx.doi.org/10.1021/jp303794s | J. Phys. Chem. B 2012, 116, 8084−8094

We performed a normal-mode analysis for the optimized geometry of KKK. The result clearly showed the CO_s mode as decoupled from both amide I modes, as proposed above. This shows that the positive Cotton band of the CO_s vibration in the VCD spectrum of KKK reflects intrinsic optical activity and is not produced by excitonic coupling. Nafie and co-workers proposed nearly 30 years ago that intramolecular hydrogen bonding produces a molecular ring structure, which provides the conduit for an electric current induced by vibrations of ring atoms. Such a current would produce a magnetic moment perpendicular to the current loop.[58] This model was later substituted by a vibronic coupling approach which yielded more localized current distributions confined to the loci of molecular vibrations.[59,60] In order to induce rotational strength the vibrating structure must be chiral. We recently provided evidence for the notion that such an effect causes the positively biased amide I′ VCD band of ionized DDD.[28] For KKK, hydrogen bonding between the ammonium group of the central lysine and the C-terminal carbonyl builds a rather large loop, which is nearly perpendicularly oriented to the C-terminal peptide group. This loop itself is too large to allow for any ring current that is not facilitated by π-bonding. The CO_s vibration alone would not be rotationally active, as observed for nearly all tripeptides that we investigated thus far.[18,19,30] However, hydrogen bonding to the carbonyl oxygen could induce optical activity if the hydrogen bond is not colinear with the CO bond, thus creating a chiral structure.[60] This is apparently the case for the CO bond in trilysine (Figure 3). The above normal mode calculation revealed a coupling between CO_s and ND bending modes of the central side chain as well as between CO_s and a COH bending vibration. Both could contribute to the mode's chirality, but it is very likely that the contribution of the latter is being averaged out because the OH bond is nearly freely rotatable around the single CO bond in the structure of Figure 3. Therefore, only the hydrogen bonding to NH_3^+ can create chirality. The VCD signal of the CO_s vibration can therefore be considered as corroborating the intrapeptide hydrogen-bonding conformation that we obtained from our structural analysis of KKK.

In this context the paper of Mikhonin et al. is noteworthy.[61] These authors used the amide III sub-band in the deep UV-resonance Raman spectra of protonated polylysine to explore the distribution of lysine residues along the ψ-coordinate. The ψ-dependence of amide III results from vibrational mixing between NH bending and CN stretching with in-plane bending mode of the preceding $C_\alpha H$ group.[62−65] They obtained a bimodal distribution of conformations, one assignable to pPII and the other one to a so-called 2.5_1-helix, which can be described as an extended β-strand conformation with $(\varphi, \psi) = (-130°, 170°)$. Such a conformation had been predicted for polylysine before by Krimm and Mark.[66] Regarding the ψ-angle, this conformation is very close to the pPII^d distribution obtained in the current study. The average φ-angle of the pPII^d subdistribution lies between the pPII and 2.5_1 distribution of Mikhonin et al.[61] We used the bimodal distribution suggested by these authors to simulate our amide I′ band profile and to calculate the above J-coupling constants. This did not lead to a satisfactory reproduction of our experimental data. The VCD-signal was underestimated, the IR-band profile was not reproduced and $^3J(H^NC^\alpha)$ as well as $^1J(NC_\alpha)$ were over-estimated. This could suggest that the average distribution of K in protonated poly-L-lysine is not completely identical with the distribution of the central residue in trilysine. However, it should be taken into consideration that the experimental methods utilized by Mikhonin et al. did not enable them to determine the φ-angles of their distributions. These authors had to assume that the two subdistributions that they obtained are assignable to canonical 2.5_1 and pPII helix conformations.

It should be noted that we carried out an earlier investigation of KKK at neutral pH, at which the N-terminal is protonated.[46] At this time we interpreted Raman, IR, and VCD amide I profiles in terms of a single, representative structure with $(\varphi, \psi) = (-50°, 170°)$. At least the ψ-coordinate is not too far away from that of the pPII^d distribution.

Temperature Dependence of KKK Conformations. Figure 4 displays the far-UV ECD spectrum of ionized KKK

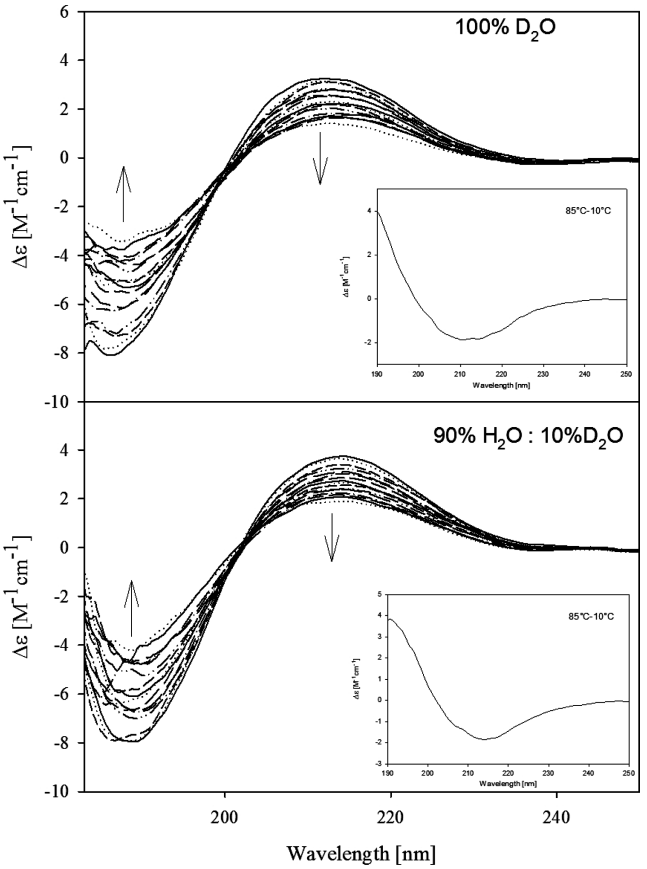

Figure 4. Ultraviolet circular dichroism spectra of trilysine in 100% D_2O (top panel) and 90% H_2O/10% D_2O (bottom panel) measured as a function of temperature. Spectra were collected at 5 °C increments from 10 to 85 °C, where the arrows indicate an increase in temperature. The insets depict the difference spectrum of 85 °C − 10 °C.

in D_2O and 90% H_2O/10% D_2O measured as a function of temperature. The measurement in the H_2O/D_2O mixture has been carried out to allow a comparison with the NMR data discussed below. All spectra exhibit a positive couplet with a positive maximum at 211 nm and a negative maximum at 186 nm. Compared with the corresponding ECD spectrum of cationic AAA, the spectrum appears somewhat blue-shifted. The negative maximum of KKK is slightly less pronounced, whereas the corresponding positive amplitude is stronger. These differences indicate that the structure of the dominant fraction deviates somewhat from the canonical pPII, in agreement with the above conformational analysis. Changing

dx.doi.org/10.1021/jp303794s | J. Phys. Chem. B 2012, 116, 8084−8094

the solvent from D_2O to 90% H_2O/10% D_2O just slightly increases the negative maximum. Corresponding spectra in Figure 4 seem to exhibit isodichroic points. A closer inspection, however, reveals that the spectra measured at high temperatures do not actually go through the isodichroic point formed by the spectra measured at lower temperature. This indicates a minor departure from a two-state behavior at high temperatures. Figure 5 depicts the temperature dependence of the

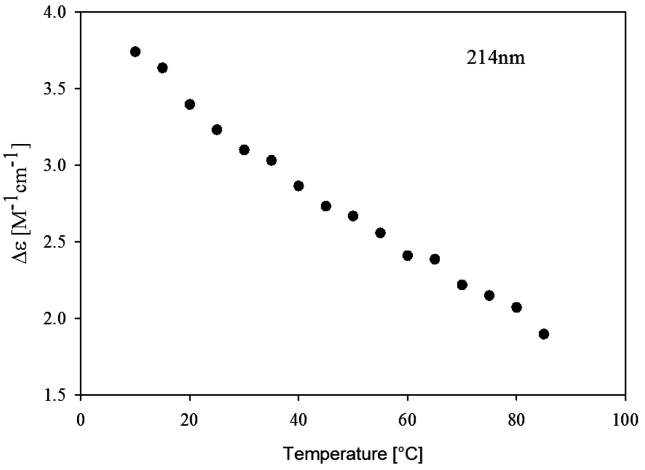

Figure 5. The $\Delta\varepsilon$ value of trilysine in 90% H_2O/10% D_2O measured at 214 nm as a function of temperature.

dichroism value measured at 214 nm. The relationship seems to be linear, but again a closer inspection reveals a deviation from linearity at higher temperature.

Figure 6 shows the temperature dependence of the $^3J(H^NN^\alpha)$ constants of the C- and N-terminal amide proton. In line with

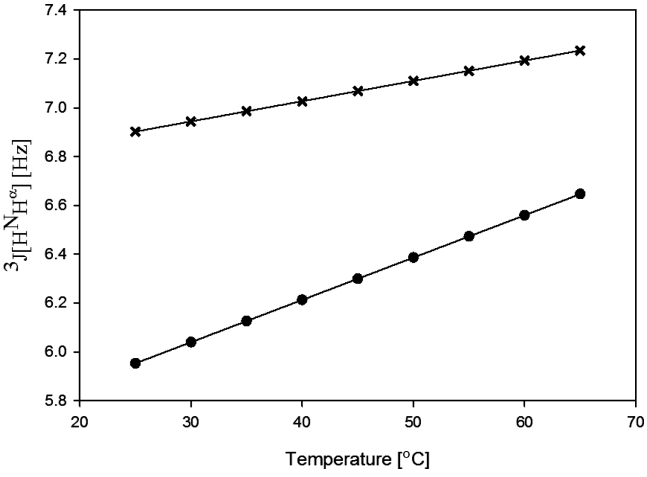

Figure 6. The $^3J(H^NH^\alpha)$ coupling constants of the N-terminal (×) and the C-terminal amide proton (●) plotted as a function of temperature.

Oh et al.,[67] we designate the amide proton of the N-terminal peptide as N-terminal amide proton and the amide proton of the C-terminal amide proton as C-terminal proton. The coupling constant reflecting the central residue shows a much weaker temperature dependence than what has been obtained, for example, for trialanine,[45] whereas the coupling constant of the C-terminal shows a normal behavior in this regard. For this peptide, we invoked a simple two-state model to self-consistently analyze the temperature dependencies of both circular dichroism and $^3J(H^NN^\alpha)$.[45] Here, we refrain from such a quantitative approach, since it is difficult to access the contribution of the obtained turn conformations to the respective experimental values. Qualitatively, two models can be invoked. If we assume a single subdistribution to exist at the upper border of the upper right-handed quadrant (or lower border of the lower left-handed quadrant), the temperature dependence of $\Delta\varepsilon$ and $^3J(H^NN^\alpha)$ would reflect a decrease of the turn fractions, which have significantly lower $^3J(H^NN^\alpha)$ values than pPII[d]. For this model to be valid, one has to assume that the turn structures give rise to a pPII-like CD spectrum, the amplitude of which has to be larger than that of the dominant pPII[d] lysine conformation. If we utilize the distribution with the bimodal subdistribution in the upper left quadrant, we could expect that the pPII-like conformation gets destabilized in favor of the more β-strand-like conformation. Even in this case, a "melting" of the β-turn conformations must contribute to the temperature dependence of $\Delta\varepsilon$ and $^3J(H^NN^\alpha)$. The temperature dependence of the C-terminal, however, is more likely to reflect a stabilization of the β-strand structure at the expense of both pPII and helical conformation. It should be emphasized that such a conformational redistribution would contribute significantly to the temperature dependence of $\Delta\varepsilon$.

The temperature coefficients of the amide protons' chemical shifts were found by using a least-squares fit to the data shown in Figure 7. The temperature coefficient associated with N-

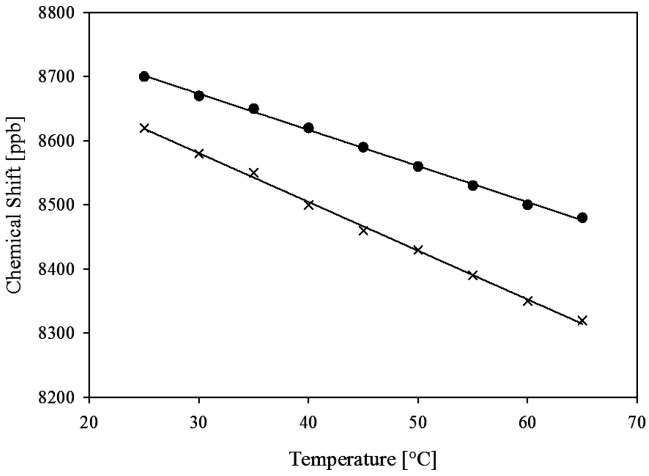

Figure 7. Chemical shifts of the N-terminal (×) and the C-terminal amide proton (●) plotted as a function of temperature. The data were fit with least-squares linear fit in SigmaPlot. The temperature coefficient associated with the N-terminal amide proton was found to be −7.6 ppb/K, and the temperature coefficient associated with the C-terminal lysine amide proton was found to be −5.63 ppb/K.

terminal lysine proton is −7.6 ppb/K, and the coefficient associated with the C-terminal proton is slightly lower at −5.8 ppb/K. These values are normally associated with amide proton resonances of statistical-coil peptides in water.[68] The amide protons are not efficiently protected from the solvent, which is consistent with the large fraction of extended conformers obtained from our analysis. Even in the minor fractions of conformation generally associated with turns, intrapeptide hydrogen bonding involving amide protons is apparently not prevalent. However, the less negative value of the temperature coefficient of the C-terminal amide proton might indicate some

dx.doi.org/10.1021/jp303794s | J. Phys. Chem. B 2012, 116, 8084−8094

short-lived hydrogen bonds in the two obtained turn structures, in which the N-terminal carbonyl oxygen and the C-terminal amide proton are ca. 2.5 Å apart (value determined with Wave function/Schrödinger software).

Conformational Analysis of OOO. Ornithine is structurally similar to lysine in that its side chain is terminated with an amino group; however, the side chain of ornithine is shorter than lysine's side chain by one methylene group. Thus, a comparison of structural distributions of trilysine and triornithine allowed us to check whether or not the length of the aliphatic segment of the basic side chain has an influence on the backbone conformation. Therefore, we analyzed the IR and VCD amide I′ profiles of triornithine, which is shown in Figure 8. Our attempt to obtain Raman profiles which were of

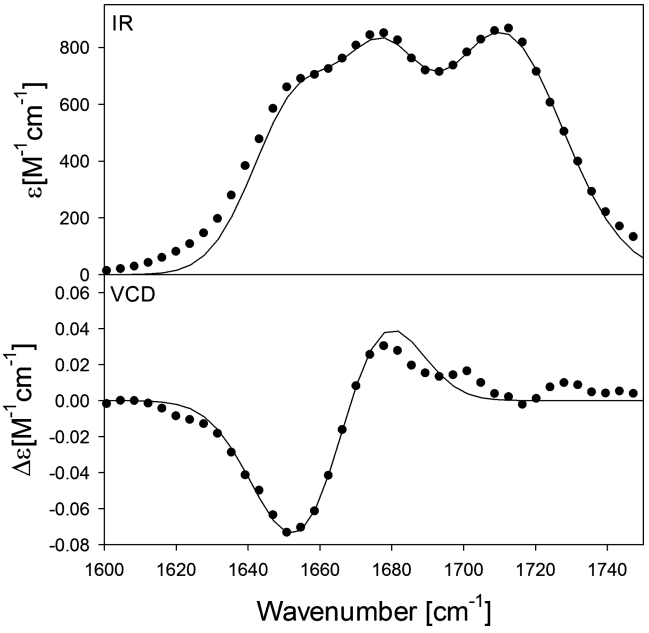

Figure 8. Amide I′ profiles of triornithine in 100% D_2O. The experimental data (black circles) and simulation (red line) of the infrared absorption (top panel) and VCD (bottom panel) are illustrated from 1600 to 1750 cm^{-1}.

sufficient quality for this type of analysis failed because the spectra were spoilt by a rather significant fluorescence dispersion and broad bands from sample impurities. Qualitatively, corresponding profiles of trilysine and triornithine are very similar. The amide I′ profiles of the latter could be reproduced by using the conformational distribution obtained for the former. Only the intrinsic frequencies of the N-terminal and the C-terminal band of triornithine had to be increased by 2 cm^{-1}. Moreover, we had to assume a stronger magnetic transition moment of 2.5×10^{-23} esu cm for the C-terminal amide I. The solid line in Figure 8 shows the result of the simulation, which is in great agreement with the experimental data. This analysis suggests that the conformational distribution of the central residue of triornithine is very similar to that of trilysine. This notion is further confirmed by DFT calculations in vacuo, which yielded a structure very similar to that obtained for KKK with dihedral angles of $(\varphi, \psi) = (69°, 168°)$. This conformation is shown in Figure 9. As observed for KKK from our DFT calculations, this conformation exhibits the ammonium group of the first and second lysine in hydrogen bonding distance to the N-terminal peptide CO and the C-terminal CO group, respectively. One would expect that this again induces optical activity into the COs vibration. The VCD spectrum in Figure 8 indicates that this might indeed be the case, but the signal-to-noise of this spectrum does not allow an unambiguous identification of such a band.

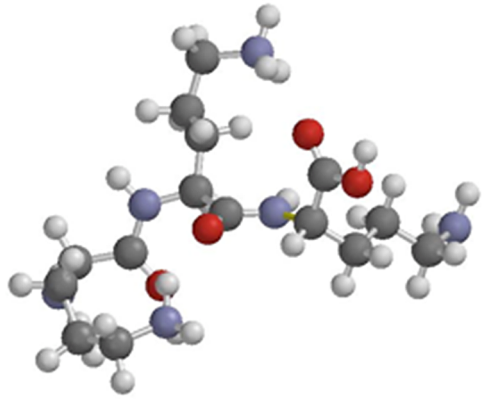

Figure 9. Structure of an unblocked OOO obtained by carrying out an in vacuo energy minimization with a DFT calculation on the B3LYP 6-31G** level of theory using the TITAN software package from Schrödinger, Inc. For this calculation, the center of the above $pPII^d$ subdistribution was used as starting point.

CONCLUSIONS

Our combined analysis of amide I′ profiles and *J*-coupling constants of protonated trilysine revealed that the conformational distribution of the central residue predominantly adopts a conformation that can be characterized as a deformed pPII structure. It is less extended than the canonical pPII conformation. Computational evidence is provided for the possibility that $pPII^d$ is stabilized by intramolecular hydrogen bonding between the side chains and peptide carbonyls. In that regard, KKK and most likely also OOO share a similarity with protonated GDG and DDD, which were recently found to form asx-like turns in solution.[18,28] Our study again underscores the notion that nearest neighbor interactions particularly between charged residues can lead to significant modifications of conformational distributions in unfolded peptides.

Generally, the results of this study show again that the classical random coil model, which assumes a nearly equal population of a broad region in the upper left quadrant and the helical region of the Ramachandran plot, is inadequate in that it neither describes the distribution sampled by amino acid residues in unfolded peptides nor the diversity of these distributions.[18,19] The very concept of a random coil is inevitably linked to the so-called isolated pair hypothesis, which stipulates that the conformational distribution of an amino acid residue is insensitive to the nature and conformation of its neighbors.[10] Results of this and preceding studies show that neighbors can have a substantial impact on conformational distributions.[28,31,33,69,70]

Apparently, nearest neighbor interactions in trilysine predominantly involves the above-discussed hydrogen-bonding pattern. The results of the DFT calculation (Figure 3) suggest that a very bent conformation of the N-terminal lysine brings its ammonium group in hydrogen-bonding contact with both peptide carbonyls (2.1 and 2.3 Å). This certainly constrains the dihedral angle of the central residue. Hydrogen bonding between the ammonium group of the central residue and the C-terminal carbonyl group should affect the central and the C-

dx.doi.org/10.1021/jp303794s | J. Phys. Chem. B 2012, 116, 8084−8094

terminal residue. This model does not necessarily conflict with the more normal conformational distribution that we obtained for the latter. The absence of a more upstream neighbor allows the C-terminal group more flexibility, and it is certainly not locked in the conformation shown in Figure 3.

The question arises why the lysine residue in GKG shows a more normal behavior, i.e., a mixture of a normal pPII and β-strand. The first reason is the absence of the N-terminal lysine and its restriction on the central lysine's conformation. The latter could still interact with the C-terminal CO group. However, this would likely bring about a high entropic cost because of the conformational flexibility of the glycine residue.

Intrinsically disordered proteins and peptides show a disproportionate fraction of charged residues such as lysine and glutamic acid.[71,72] It is obvious that their charges contribute to the stability of their unfolded state. In addition, the results in the present study suggest that they are able to create local order. Moreover, as shown recently, protonated aspartic residues can sample a variety of turnlike structures.[18,28] In foldable proteins this makes this amino acid residue an ideal candidate for the initiation of folding. In its deprotonated state, however, triaspartic acid shows a mixture of canonical pPII and pPII^d/β-strand conformations, which are also stabilized by intrapeptide hydrogen bonding.[28] Ionized lysine looks to some extent like a mixture of protonated and ionized aspartic acid; it should be able to facilitate turns as well as the temporary formation of rather extended segments with pPII^d structure. Thus, depending on their protonation state, residues like aspartic acid and lysine (and most likely also glutamic acid) can facilitate a more compact structure of unfolded peptides and proteins. Something like this occurs in the frequently investigated Ac–$X_2(A)_7O_2$–NH_2 (XAO; X and O denote 2,4-diaminobutyric acid and ornithine, respectively), where X, which can be regarded as the next lower homologue of O, samples turns and induces some turn propensity into the distribution of the N-terminal alanine.[20,73,74] As a consequence, the radius of gyration of the peptide is much shorter than it would be if all residues were sampling only extended conformations.[20,75]

While the population of turns can cause compact structures in longer peptides and proteins, the sampling of pPII or pPII^d could in principle cause the formation of extended stretches and thus a high degree of local order. The use of terms like 3_1 or 2.5_1 helix seem to point in this direction.[37] Generally, however, the prospect for such a scenario to occur seems to be greatly diminished owing to the lack of any evidence for the existence of stable, cooperatively formed structures in unfolded peptides and proteins including poly-L-lysine. If one assumes the obtained statistical weight of 0.7 for pPII^d, the probability for a segment of six lysines to form a pPII^d-like helix (which lies somewhere between 3_1 and 2.5_1) is approximately 0.12. This probability is small but not negligible. One would expect this conformation to be short-lived and exchange with shorter segments interrupted by turns that will be further favored by their higher combinatorial entropy. However, the above proposed structure with side chain–(C-terminal) carbonyl hydrogen bonding inferred from DFT calculations can potentially restrict the sampling space of its neighbors. Upon further inspection of oligolysines, it is apparent that if the third residue adopts the type II β-like conformation obtained from our analysis of KKK and the preceding residues are in the pPII^d conformation, the third downstream lysine side chain clashes with the first side chain. This could be the reason for the absence of this conformation in the distribution of the C-terminal residue of the peptide. For $(K)_n$-segments with $n > 3$, the side chains of the fourth, fifth, etc. residue would clash with the side chains of the first, second, third, etc. residue, if the former adopted type IV/I′ conformations as defined in this study and the latter sample pPII^d. This suggests that long poly-L-lysine segments can adopt turn structures only at their second residue, and even this requires that the side chain of the preceding residues are not too sterically demanding. In other words: lysine in pPII^d forces downstream residues of a polylysine segment into pPII^d. Thus, 2.5_1- or 3_1-like helices could indeed become much more stable than expected from just the local propensities for this conformation.

A word of caution seems to be appropriate here. All DFT calculations reported in this study were performed in vacuo, thus neglecting the competing forces of water with regard to hydrogen bonding. One might therefore argue that water is likely to destabilize or even prevent hydrogen bonding between the ammonium group and the C-terminal carbonyl. However, on the other side the rather unusual magnetic transition moment of the C-terminal carbonyl stretching mode seems to indicate that such a hydrogen bond really exists. We propose that that steric constraints in pPII^d force the lysine side chain into a conformation in which the ammonium group is in close proximity of the C-terminal carbonyl group, thus facilitating the formation of side chain–C-terminal hydrogen bond, which in turn stabilizes the pPII^d.

The situation is less restrictive for aspartic acid owing to its much shorter side chain. We therefore conclude that while motifs rich in aspartic acid (DDD, DxD, etc.) are likely to promote turn formations and compact structures, lysine-rich motifs are more likely to form rather stable extended, left-helical structures. Whether this can facilitate the binding of disordered proteins with lysine-rich segments[38,40,41] to targets like DNA or RNA remains to be seen.

■ ASSOCIATED CONTENT

Supporting Information

The isolation of the magnetic transition dipole moment contribution to the amide I′ VCD band profile of KKK and the structure of KKKG obtained from DFT structure optimization. This material is available free of charge via the Internet at http://pubs.acs.org.

■ AUTHOR INFORMATION

Corresponding Author

*Phone: 215-895-2268. Fax: 215-895-1265. E-mail: rschweitzer-stenner@drexel.edu.

Notes

The authors declare no competing financial interest.

■ ACKNOWLEDGMENTS

This research was supported by an NSF grant (Chem 0804492), and an REU supplement (Chem 0939972) to R.S.S. D.J.V. thanks Andrew Hagarman and Thomas Measey for altruistic support at the early stage of the project. R.S.S. thanks Laurence Nafie for very helpful information about the origin of magnetic transition dipole moments and for sending us some of the papers cited in this paper.

■ REFERENCES

(1) Schweitzer-Stenner, R. *Mol. BioSyst.* **2012**, *8*, 122–133.

(2) Shi, Z.; Shen, K.; Liu, Z.; Kallenbach, N. R. *Chem. Rev.* **2006**, *106*, 1877−1897.
(3) DeBartolo, J.; Jha, A.; Freed, K., F.; Sosnick, T. R. In *Proteins and Peptides. Folding, Misfolding and Unfolding*; Schweitzer-Stenner, R., Ed.; Wiley & Sons: Chichester, 2012; pp 79−98.
(4) Alexandrescu, A. T.; Abeygunawardana, C.; Shortle, D. *Biochemistry* **1994**, *33*, 1063−1072.
(5) Shortle, D. *Adv. Protein Chem.* **2002**, *62*, 1−23.
(6) Meier, S.; Grzesiek, S.; Blackledge, M. *J. Am. Chem. Soc.* **2007**, *129*, 9799−9807.
(7) Mukrasch, M. D.; Markwick, P.; Biernat, J.; von Bergen, M.; Bernado, P.; Greisinger, C.; Mandelkow, E.; Zweckstetter, M.; Blackledge, M. *J. Am. Chem. Soc.* **2007**, *129*, 5235−5243.
(8) Ramachandran, G. N.; Ramachandran, C.; Sasisekharan, V. *J. Mol. Biol.* **1963**, *7*, 95−99.
(9) Brant, D. A.; Flory, P. J. *J. Am. Chem. Soc.* **1965**, *87*, 2791−2800.
(10) Flory, P. J. *Statistical Mechanics of Chain Molecules*; Wiley & Sons: New York, 1969.
(11) Tanford, C. *Adv. Protein Chem.* **1968**, *23*, 121−282.
(12) Shi, Z.; Chen, K.; Liu, Z.; Ng, A.; Bracken, W. C.; Kallenbach, N. R. *Proc. Natl. Acad. Sci. U. S. A.* **2005**, *102*, 17964−17968.
(13) Shi, Z.; Olson, C. A.; Rose, G. D.; Baldwin, R. L.; Kallenbach, N. R. *Proc. Natl. Acad. Sci. U. S. A.* **2002**, *99*, 9190−9195.
(14) Shi, Z.; Woody, R. W.; Kallenbach, N. R. *Adv. Protein Chem.* **2002**, *62*, 163−240.
(15) Poon, C. D.; Samulsi, E. T.; Weise, C. F.; Weisshaar, J. C. *J. Am. Chem. Soc.* **2000**, *122*, 5612−5613.
(16) Weise, C. F.; Weisshaar, J. C. *J. Phys. Chem. B* **2003**, *107*, 3265.
(17) Graf, J.; Nguyen, P. H.; Stock, G.; Schwalbe, H. *J. Am. Chem. Soc.* **2007**, *129*, 1179−1189.
(18) Hagarman, A.; Mathieu, D.; Toal, S.; Measey, T. J.; Schwalbe, H.; Schweitzer-Stenner, R. *Chem.—Eur. J.* **2011**, *17*, 6789−6797.
(19) Hagarman, A.; Measey, T. J.; Mathieu, D.; Schwalbe, H.; Schweitzer-Stenner, R. *J. Am. Chem. Soc.* **2010**, *132*, 540−551.
(20) Schweitzer-Stenner, R.; Measey, T. *Proc. Natl. Acad. Sci. U. S. A.* **2007**, *104*, 6649−6654.
(21) Verbaro, D.; Ghosh, I.; Nau, W. M.; Schweitzer-Stenner, R. *J. Phys. Chem. B* **2010**, *114*, 17201−17208.
(22) Serrano, L. *J. Mol. Biol.* **1995**, *254*, 322−333.
(23) Swindells, M. B.; MacArthur, M. W.; Thornton, J. M. *Nat. Struct. Biol.* **1995**, *2*, 596−603.
(24) Jha, A. K.; Colubri, A.; Zaman, M. H.; Koide, S.; Sosnick, T. R.; Freed, K. F. *Biochemistry* **2005**, *44*, 9691−9702.
(25) Jha, A. K.; Kolubri, A.; Freed, K. F.; Sosnick, T. R. *Proc. Natl. Acad. Sci. U. S. A.* **2005**, *102*, 13099−13104.
(26) Shi, Z. S.; Chen, K.; Liu, Z. G.; Sosnick, T. R.; Kallenbach, N. R. *Proteins—Struct. Funct. Bioinf.* **2006**, *63*, 312−321.
(27) Zaman, M. H.; Shen, M.-Y.; Berry, R. S.; Freed, K. F.; Sosnick, T. R. *J. Mol. Biol.* **2003**, *331*, 693−711.
(28) Duitch, L.; Toal, S.; Measey, T. J.; Schweitzer-Stenner, R. *J. Phys. Chem. B* **2012**, *116*, 5160−5171.
(29) Eker, F.; Cao, X.; Nafie, L.; Griebenow, K.; Schweitzer-Stenner, R. *J. Phys. Chem. B* **2003**, *107*, 358−365.
(30) Eker, F.; Cao, X.; Nafie, L.; Schweitzer-Stenner, R. *J. Am. Chem. Soc.* **2002**, *124*, 14330−14341.
(31) Schweitzer-Stenner, R. *J. Phys. Chem. B* **2009**, *113*, 2922−2932.
(32) Schweitzer-Stenner, R.; Measey, T.; Hagarman, A.; Dragomir, I. In *Vibrational Spectroscopy on Peptides and Proteins*; Longhi, S., Uversky, V. N., Eds.; Wiley & Sons: Chichester, 2009; pp 171−224.
(33) Pizanelli, S.; Forte, C.; Monti, S.; Zandomeneghi, G.; Hagarman, A.; Measey, T. J.; Schweitzer-Stenner, R. *J. Phys. Chem. B* **2010**, *114*, 3965−3978.
(34) Tiffany, M. L.; Krimm, S. *Biopolymers* **1968**, *6*, 1767−1770.
(35) Dukor, R.; Keiderling, T. A. *Biopolymers* **1991**, *31*, 1761.
(36) Rucker, A. L.; Creamer, T. P. *Protein Sci.* **2002**, *11*, 980−985.
(37) Mikhonin, A. V.; Myshakina, N., S.; Bykov, S. V.; Asher, S. A. *J. Am. Chem. Soc.* **2005**, *127*, 7712−7720.
(38) Loewen, C. A.; Lee, S. M.; Shin, Y.-K.; Reist, N. E. *Mol. Cell. Biol. Cell* **2006**, *17*, 5211−5226.
(39) Mace, K. E.; Biela, L. M.; Reist, M. E. *Genesis* **2009**, *47*, 337−345.
(40) Wu, L.-J.; Xu, L.-R.; Liao, J.-M.; Chen, J.; Linag, Y. *PLoS ONE* **2011**, *6*, e21929.
(41) Chang, C.-K.; Hsu, Y.-L.; Chang, Y.-H.; Chao, F.-A.; Huang, Y.-S.; Hu, C.-K.; Huang, T.-H. *J. Virol.* **2008**, *83*, 2264.
(42) Schweitzer-Stenner, R.; Measey, T.; Kakalis, L.; Jordan, F.; Pizzanelli, S.; Forte, C.; Griebenow, K. *Biochemistry* **2007**, *46*, 1587−1596.
(43) Glasoe, P. K.; Long, F. A. *J. Phys. Chem.* **1960**, *64*, 188.
(44) Jentzen, W.; Unger, E.; Karvounis, G.; Shelnutt, J. A.; Dreybrodt, W.; Schweitzer-Stenner, R. *J. Phys. Chem.* **1995**, *100*, 14184−14191.
(45) Toal, S.; Omidi, A.; Schweitzer-Stenner, R. *J. Am. Chem. Soc.* **2011**, *133*, 12728−12739.
(46) Eker, F.; Griebenow, K.; Cao, X.; Nafie, L.; Schweitzer-Stenner, R. *Biochemistry* **2004**, *43*, 613−621.
(47) Woutersen, S.; Hamm, P. *J. Phys. Chem. B* **2000**, *104*, 11316−11320.
(48) Torii, H.; Tasumi, M. *J. Raman Spectrosc.* **1998**, *29*, 81−86.
(49) Schweitzer-Stenner, R. *J. Phys. Chem. B.* **2004**, *108*, 16965−16975.
(50) Kubelka, J.; Kim, J.; Bour, P.; Keiderling, T. A. *Vibr. Spectrosc.* **2007**, *42*, 63−73.
(51) Kubelka, J.; Silva, R. A. G. D.; Keiderling, T. A. *J. Am. Chem. Soc.* **2002**, *124*, 5325−5332.
(52) Sen, A. C.; Keiderling, T. A. *Biopolymers* **1984**, *23*, 1533−1545.
(53) Wirmer, J.; Schwalbe, H. *J. Biomol. NMR* **2002**, *23*, 47−55.
(54) Schweitzer-Stenner, R. *Biophys. J.* **2002**, *83*, 523−332.
(55) Woutersen, S.; Hamm, P. *J. Chem. Phys.* **2001**, *114*, 2727−2737.
(56) Measey, T.; Hagarman, A.; Eker, F.; Griebenow, K.; Schweitzer-Stenner, R. *J. Phys. Chem. B* **2005**, *109*, 8195−8205.
(57) Eker, F.; Griebenow, K.; Cao, X.; Nafie, L.; Schweitzer-Stenner, R. *Proc. Natl. Acad. Sci. U. S. A.* **2004**, *101*, 10059.
(58) Nafie, L. A.; Oboodi, M. R.; Freedman, T. B. *J. Am. Chem. Soc.* **1983**, *105*, 7449−7450.
(59) Nafie, L. A. *J. Phys. Chem. A.* **1997**, *101*, 7826−7833.
(60) Gigante, D. M. P.; Long, F.; Bodack, L. A.; Evans, J. M.; Kallmerten, J.; Nafie, L. A.; Freedman, T. B. *J. Phys. Chem. A.* **1999**, *103*, 1523−1537.
(61) Ma, L.; Ahmed, Z.; Mikhonin, A. V.; Asher, S. A. *J. Phys. Chem. B* **2007**, *111*, 7675−7680.
(62) Asher, S. A.; Ianoul, A.; Mix, G.; Boyden, M. N.; Karnoup, A.; Diem, M.; Schweitzer-Stenner, R. *J. Am. Chem. Soc.* **2001**, *123*, 11775−11781.
(63) Lord, R. *Appl. Spectrosc.* **1977**, *31*, 187−194.
(64) Schweitzer-Stenner, R.; Eker, F.; Huang, Q.; Griebenow, K.; Mroz, P. A.; Kozlowski, P. M. *J. Phys. Chem. B* **2002**, *106*, 4294−4304.
(65) Mikhonin, A. V.; Ahmed, Z.; Ianoul, A.; Asher, S. A. *J. Phys. Chem. B* **2004**, *108*, 19020−19028.
(66) Krimm, S.; Mark, J. E. *Proc. Natl. Acad. Sci. U. S. A.* **1968**, *60*, 1122−1129.
(67) Oh, K.-I.; Lee, K.-K.; Park, E. K.; Kwang, G. S.; Cho, M. *Chirality* **2010**, *22*, E186−E201.
(68) Mertuka, G.; Dyson, H. J.; Wright, P. E. *J. Biomol. NMR* **1995**, *5*, 14−24.
(69) Schweitzer-Stenner, R.; Gonzales, W.; Bourne, J. T.; Feng, J. A.; Marshall, G. A. *J. Am. Chem. Soc.* **2007**, *129*, 13095−13109.
(70) Chen, K.; Liu, Z.; Zhou, C.; Shi, Z.; Kallenbach, N. R. *J. Am. Chem. Soc.* **2005**, *127*, 10146−10147.
(71) Uversky, V. N. In *Unfolded Proteins. From Denaturated to Intrinsically Disordered*; Creamer, T. P., Ed.; Nova: Nauppauge, NY, 2008; pp 237−294.
(72) Dunker, A. K.; Lawson, J. D.; Brown, C. J.; Williams, R. M.; Romero, P.; Oh, J. S.; Oldfield, C. J.; Campen, A. M.; Ratliff, C. M.; Hipps, K. W.; Ausio, J.; Nissen, M. S.; Reeves, R.; Kang, C.; Kissinger, C. R.; Bailey, R. W.; Griswold, M. D.; Chiu, W.; Garner, E. C.; Obradovic, Z. *J. Mol. Graphics Modell.* **2001**, *19*, 26−59.

(73) Makowska, J.; Rodziewicz-Motowidlo, S.; Baginska, K.; Vila, J. A.; Liwo, A.; Chmurzynski, L.; Scheraga, H. A. *Proc. Natl. Acad. Sci. U.S.A.* **2006**, *103*, 1744−1749.
(74) Chen, K.; Liu, Z.; Zhou, C.; Bracken, W. C.; Kallenbach, N. R. *Angew. Chem. Int. Ed.* **2007**, *46*, 9036−9039.
(75) Zagrovic, B.; Lipfert, J.; Sorin, E. J.; Millett, I. S.; van Gunsteren, W. F.; Doniach, S.; Pande, V. S. *Proc. Natl. Acad. Sci. U. S. A.* **2005**, *102*, 11698−11703.